1904

ACOUSTO-OPTIC ATTENUATION FILTERS BASED ON TAPERED OPTICAL FIBRES

R. Feced, C. Alegria, M.N. Zervas, R.I. Laming

Optoelectronics Research Centre

University of Southampton

Southampton SO17 1BJ

Tel: 44- (0)1703 - 593141 Fax: 44- (0)1703 - 593142

IE^3 JOURNAL OF SELECTED TOPICS IN QUANTUM ELECTRONICS APPEAR AUTUMN

ACOUSTO-OPTIC ATTENUATION FILTERS BASED ON TAPERED OPTICAL FIBRES

Abstract

This paper studies the acousto-optic interaction induced by an acoustic flexural wave among the optical propagation modes supported by tapered optical fibres. We have investigated the evolution of the acousto-optic resonance condition as the fibre is progressively tapered, showing that the taper radius can be regarded as a new degree of freedom in the design of acousto-optic filters. Finally, we demonstrate a novel acousto-optic filter based on nonuniform tapers for dynamic gain flattening of optical fibre amplifiers.

1. INTRODUCTION

The acousto-optic (AO) effect in optical fibres has been applied to the design of many practical devices, ranging from tunable filters, frequency shifters and equalisers to optical switches and modulators [1-14]. All these devices rely on the selective coupling that an acoustic wave induces among the propagation modes of an optical fibre. Many different schemes have already been considered depending on the nature of the acoustic waves and the optical modes involved. In the early all-fibre AO devices, a flexural acoustic wave was used to couple the fundamental mode (LP_{01}) to the first higher order mode (LP_{11}) of a dual-mode optical fibre [2-4,8]. Other implemented AO devices were based on coupling among the modes of a dual-core optical fibre [5], or the polarisation modes of a high birefringent fibre [1,6-7]. In all these devices, the optical modes that interacted with the acoustic wave were guided by the core of the optical fibre.

The use of the AO effect in tapered fibre structures (null couplers, fibre tapers etc.) has given rise to a whole new family of AO devices [9-14]. In this case, the AO interaction occurs between the optical modes supported by a thin silica taper waist with radius of a few microns. These modes can be considered as cladding modes because the residual core does not play any role in the propagation. One of the main advantages of the tapered AO devices is their low radio-frequency power consumption. This is a consequence of the concentrator effect that the tapered fibre has on the acoustic waves.

More recently, novel AO filters that couple light from the fundamental guided mode (LP_{01}) of a single-mode optical fibre to several low order cladding modes (LP_{11}, LP_{12}, etc.) through an acoustic flexural wave have attracted wide interest [15-16]. As the loss spectrum of these filters can be dynamically controlled, they are suitable for flattening the gain profile of optical fibre amplifiers. The major advantage of AO filters with respect to their static counterparts, e.g. long-period gratings [17], is that they are reconfigurable and can compensate for gain saturation effects caused by power fluctuations of the input signal [15-16]. The tunability of the AO filters is due to the dependence of the resonance wavelength on the frequency of the acoustic waves. Filters with complex loss spectrum have been synthesised by driving the acoustic transducer with several radio-frequency tones of different amplitudes and frequencies [15-16].

In this paper we investigate the effects of a controlled fibre tapering on the coupling between the fundamental and the low order cladding modes of the AO filter. It is well recognised that the control of the radius profile along a nonuniformly tapered fibre can be regarded as an extra degree of freedom for tailoring the spectral characteristics of the filter. One potential advantage of this approach is that the requirement of multiple radio-frequency (RF) synthesisers to drive the acoustic transducer can be avoided, simplifying the implementation of the AO filter.

The paper is structured as follows. In Section 2, we analyse theoretically the AO resonance conditions and coupling efficiencies among the modes of tapered fibres. We will describe the evolution of the resonance conditions as the fibre diameter is varied. In Section 3, this study is confirmed by experimental measurements in fibres tapered to various degrees. We also demonstrate the application of AO filters based on nonuniform tapers as gain equalisers for optical fibre amplifiers. The design consists of two AO filters driven by a single electrical frequency and with spectral characteristics determined by the taper profile. When these two filters are cascaded, the amplified spontaneous emission (ASE) of an erbium doped fibre amplifier (EDFA) is flattened to within 1dB over a spectral range of 30nm for a large range of input saturating signals.

2. THEORY

The principle of operation of the AO filter studied in this work is shown in Figure 1. A flexural acoustic wave is excited in a tapered single mode (SM) optical fibre and, as it propagates, induces coupling among the optical modes supported by the fibre. The single mode fibre has been tapered along its length to modify the propagation properties of the acoustic and optical modes, tailoring the coupling among them.

In this section we will first describe the acoustic and optical modes involved in the AO interaction in SM tapered fibres, and then the possible resonance conditions between them. Two extreme cases have already been described in the literature. The first one, studied by Kim et al[15-16], corresponds to untapered fibres. In this case coupling was observed between the fundamental core-guided mode and several cladding modes of the fibre. In the other case, examined by Birks et al[9-14], the fibre was tapered to a very thin waist of few microns. In this tapering range the coupled optical modes can be regarded as cladding modes supported by the silica waist. Here we investigate the evolution of the AO resonance condition between these two extreme cases. We show that, in general, two resonance optical wavelengths exist for a given frequency of the acoustic wave, radius of the taper, and pair of interacting optical modes. We also study how the coupling efficiency among the optical modes evolves as a function of the tapering.

2.1 ACOUSTIC FLEXURAL WAVES IN TAPERED FIBRES

The propagation of acoustic flexural waves in thin fibres has been extensively discussed in the literature [4]. If the wavelength of the acoustic wave is much longer than the fibre diameter, the first flexural mode is well described by the Bernoulli-Euler approximation. For a tapered fibre, the equation of propagation for the deflection of the neutral axis (ξ) is derived from the Lagrangian density:

$$L(z)=\frac{1}{2}\rho\,A(z)\left(\frac{\partial\xi(z,t)}{\partial t}\right)^2-\frac{1}{2}Y\,I(z)\left(\frac{\partial^2\xi(z,t)}{\partial^2 z}\right)^2-\frac{1}{2}T\left(\frac{\partial\,\xi(z,t)}{\partial\,z}\right)^2 \qquad (1)$$

where ρ is the fibre density; $A(z)$ is the local cross-section along the taper; Y is the Young modulus; T is the tension to which the fibre is subjected. $I(z)$ is the local moment of inertia that for a cylindrical rod is given by:

$$I(z)=\frac{\pi\,(b(z))^4}{4} \qquad (2)$$

where b(z) is the local radius along the taper. The last two terms of this Lagrangian density account for the restoring forces that act on the fibre, i.e. stiffness and tension. The effect of tension is much smaller than that of stiffness, and can be taken as a perturbation in the analysis.

Assuming that the flexural wave propagates adiabatically along the tapered fibre and that is not subjected to tension (T=0), the deflection of the neutral axis $\xi(z,t)$ predicted by (1) is given by:

$$\xi(z,t)=\frac{\tilde{\xi}(z)}{2}e^{-j\int_0^z K(\eta)d\eta}e^{j\Omega t}+c.c=\left\{\frac{\xi_o}{2}\left(\frac{K(z)}{K(0)}\right)^{5/2}e^{-\int_0^z \alpha(\eta)d\eta}\right\}e^{-j\int_0^z K(\eta)d\eta}e^{j\Omega t}+c.c. \tag{3}$$

where $\tilde{\xi}(z)$ is the envelope amplitude of the deflection, ξ_o is the peak deflection at the initial position (z=0), Ω is the acoustic angular frequency, $\alpha(z)$ is a phenomenological damping constant, and c.c. stands for complex conjugate. K(z) is the local acoustic propagation constant along the taper, given by:

$$K(z)=\frac{2\pi}{\Lambda(z)}=\sqrt{\frac{2\,\Omega}{c_{ext}\,b(z)}} \tag{4}$$

where $\Lambda(z)$ is the local acoustic wavelength and c_{ext} is the extensional acoustic velocity ($\sqrt{Y/\rho}$) for silica glass. If the fibre is subjected to a tension T, the last term of the Lagrangian density has to be considered, and the acoustic propagation constant will be perturbed according to:

$$\frac{\delta K(z)}{K(z)}=-\frac{T}{4\Omega}\frac{c_{ext}}{Y}\frac{1}{\sqrt{A(z)\,I(z)}} \tag{5}$$

The main reason for analysing the propagation of the acoustic wave is to predict its effect on the electromagnetic properties of the fibre. The acousto-optic interaction is usually expressed in terms of the longitudinal strain distribution along the fibre $S_{zz}(r,\phi,z,t)$:

$$S_{zz}(r,\phi,z,t) = -\frac{\partial^2 \xi}{\partial z^2} r\cos\phi \approx K(z)^2 \frac{\tilde{\xi}(z)}{2} e^{-j\int_0^z K(\eta)d\eta} e^{j\Omega t} r\cos\phi + c.c. \tag{6}$$

where r and ϕ are the radial and angular cylindrical coordinates. Further discussion follows in Section 2.3

2.2 OPTICAL MODES

A single-mode optical fibre with finite cladding supports cladding-modes which are primarily guided by the entire cladding/air structure. The effective refractive index for these modes has as upper bound the refractive index of the cladding and as lower bound the air refractive index. The AO interaction under study involves coupling between the fundamental LP_{01} mode and several low order odd cladding modes LP_{1m} (m=1,2,3) in a tapered fibre. If the taper is smooth, these modes will evolve adiabatically, maintaining their identity with insignificant losses during their propagation. Mathematically, the electric field of a multimode optical wave that propagates along a gradually tapered fibre can be represented as:

$$\vec{E}(r,\phi,z,t) = \sum_{mn} \frac{A_{mn}(z)}{2} \vec{E}_{mn}(r,\phi,b(z)) e^{-j\int_0^z \beta_{mn}(\eta)d\eta} e^{j\omega_{mn}t} + c.c. \tag{7}$$

where $\beta_{mn}(z)$ is the propagation constant of the mode LP_{mn}, ω_{mn} is its angular frequency, $\vec{E}_{mn}(r,\phi,b(z))$ is its normalised field pattern, and $A_{mn}(z)$ is a slowly varying complex amplitude. In (7) we have assumed different angular frequencies for each optical mode, as is the case when they are coupled through an AO interaction. Both $\beta_{mn}(z)$ and $\vec{E}_{mn}(r,\phi,b(z))$ depend on the radius of the cladding and have to be considered as local propagation constants and normalised fields respectively. For adiabatic propagation without transfer of power among the modes, $A_{mn}(z)$ is a constant independent of z. We will always assume that when a fibre is tapered the aspect ratio between the dimensions of the core and cladding is maintained along the taper.

By symmetry considerations, the only modes that can exchange power with the fundamental mode (LP_{01}) through a flexural acoustic wave are the LP_{1m} cladding modes. The difference in propagation constants between every pair of interacting modes ($LP_{01} \leftrightarrow LP_{1m}$) is expressed in terms of effective beatlengths L_m:

$$L_m = \frac{2\pi}{\beta_{01} - \beta_{1m}} \tag{8}$$

Figure 2 shows the dispersion of the beatlength L_m for the first three pair of modes as a function of the normalised frequency V ($= \frac{2\pi}{\lambda} a\,NA$, with a being the core radius). These dispersion curves were calculated both by the scalar linearly-polarised mode approximation and with the exact fully vectorial model, reaching in both cases very similar conclusions. The results presented in Figure 2 correspond to the fully-vectorial calculation in which we have ignored the small splitting that appears among the modes that compose a given LP mode set. The only assumption in the calculation is that the ratio between the cladding (b) and core (a) radii is 62.5/4. The three curves show a similar behaviour. The beatlength is low for small and high values of the normalised frequency V, and exhibits a maximum for a V near to 1. For small values of V, the fundamental mode behaves as a cladding mode, not being confined by the core. The maximum corresponds roughly to the point at which the fundamental mode LP_{01} begins to be guided by the core.

The previous dispersion curves have been expressed in terms of normalised parameters to be able to predict the AO resonances in tapered fibres. In order to study the coupling strength of the AO interaction, we have also calculated the normalised field profiles $\vec{E}_{mn}(r,\phi,b(z))$ for the scalar linearly-polarised case. In this approximation the fields are transversal and obey the orthogonality condition:

$$\int_A \vec{E}_l^*(r,\phi,V)\cdot\vec{E}_k(r,\phi,V)\,dA = \delta_{kl} \tag{9}$$

where A is the fibre cross-section and δ_{kl} is the Kronecker delta, with l and k corresponding to different index sets mn. Notice that in (9) the field eigenfunctions depend on the taper radius b through the normalised frequency V.

2.3 ACOUSTO-OPTIC INTERACTION

The AO interaction in optical fibres is due to two mechanisms that give opposite contributions [3]. The main effect is due to the geometrical deformation that the flexural wave induces on the optical fibre. The second mechanism is the change in refractive index due to the elasto-optic effect. Both contributions can be incorporated into an effective change of the dielectric permitivity $\Delta\varepsilon$ of the fibre, which acts as a perturbation for the propagation equations:

$$\Delta\varepsilon(r,\phi,z,t) = 2n^2\varepsilon_0\, S_{zz}(r,\phi,z,t)\,(1-\chi) \tag{10}$$

where n is the silica refractive index; ε_0 is the vacuum permitivity; S_{zz} is the longitudinal strain given in (6); and χ is the elasto-optic coefficient. χ has a value of 0.22 at low acoustic frequencies and decreases as the fibre diameter becomes comparable to the acoustic wavelength [8].

The AO resonance condition for effective coupling between two optical modes is obtained by the usual momentum and energy conservation requirements which can be expressed as:

$$L_m(\lambda_R,b) = \Lambda(b,\Omega) \tag{11a}$$

$$\omega_m - \omega_0 = \pm\Omega \tag{11b}$$

Equation (11a) states that the beatlength L_m (8) between the interacting modes is equal to the acoustic wavelength Λ defined in (4). Equation (11b) indicates that the frequency of the LP_{1m} mode (ω_m) is shifted with respect to the fundamental mode (ω_0) by the acoustic frequency (Ω). From Equation (11a) we can calculate the resonance wavelengths λ_R as a function of the taper radius b for the three AO interactions that we have experimentally observed. The results, shown in Figure 3, indicate that the resonance wavelengths are double-branched functions of the taper radius. The short-wavelength resonance corresponds to the long-V range of beatlengths, where the fundamental mode is well guided by the core. On the other hand, the long-wavelength resonance corresponds to the low-V range, where the fundamental mode becomes a cladding mode. For practical AO devices with resonance wavelengths of about 1.5 μm, the short-wavelength resonance case has been implemented in untapered fibres [15-16], while the long-wavelength resonance has been achieved by tapering the fibres to very thin waists [9-14].

The resonance wavelength is usually tuned by means of the frequency of the acoustic wave. The effect of the acoustic frequency is opposite for both branches and can be predicted from Equation (4) and Figure 2. For the short-wavelength resonance, an increase in acoustic frequency translates into a decrease of the resonance wavelength, in contrast to the long-wavelength resonance, that would increase. A second way to tune the resonance wavelength is by subjecting the fibre to axial tension. Equation (5) and Figure 2 indicate that the effect of strain is again different for both resonance branches. If the fibre is strained, the short-wavelength resonance shifts towards longer wavelengths, while the long-wavelength resonance will decrease.

The AO induced exchange of power among the modes propagating in a tapered SM fibre is described through the coupled mode formalism. For a given pair of modes, the following set of coupled equations can be written:

$$\frac{d}{dz}A_0(z) = -j\kappa(z)\,A_m(z)\,e^{-j\int_0^z (\beta_m(\eta)-\beta_0(\eta)+K(\eta))d\eta}$$

$$\frac{d}{dz}A_m(z) = -j\kappa^*(z)\,A_0(z)\,e^{+j\int_0^z (\beta_m(\eta)-\beta_0(\eta)+K(\eta))d\eta} \tag{12}$$

where $A_0(z)$ is the amplitude of the fundamental mode LP_{01}, $A_m(z)$ is the amplitude of the cladding mode LP_{1m} and $\kappa(z)$ is the coupling coefficient. $\kappa(z)$ is calculated through an overlap integral that involves the normalised mode field patterns and the perturbation of the dielectric permitivity induced by the acoustic wave:

$$\kappa(z) = \frac{4\pi^4 n\,(1-\chi)\,\tilde{\xi}\,a}{\lambda\,\Lambda^2}\,OI_m(V) \tag{13}$$

where λ is the optical wavelength, a is the core radius, and OI_m is a normalised overlap integral that only depends on V and is defined as:

$$OI_m(V) = \frac{1}{a}\int_0^\infty \gamma_{01}^*(r,V)\,\gamma_{1m}(r,V)\,r^2\,dr \tag{14}$$

where $\gamma_{nk}(r,V)$ is the radial dependent part of the field pattern for the LP_{nk} mode:

$$\bar{E}_{nk}(r,\phi,V) = \gamma_{nk}(r,V)\cos(n\phi)\,\bar{u} \tag{15}$$

and $\bar{u}$ is a transversal unit vector.

The normalised overlap integral OI_m as a function of the normalised V has been represented in Figure 4. It can be observed that there are three regions with very different behaviour. For low values of V, both the fundamental and the three cladding modes considered are not confined by the core. In this case the radial part of the LP_{01} mode only overlaps efficiently with the radial part of the LP_{11} mode, while the LP_{12} and LP_{13} modes are almost orthogonal to the LP_{01}. At very high values of V the guiding effect of the core becomes increasingly important, confining the modes in a very small region around it. In this case, the radial part of the LP_{01} mode overlaps again well with the LP_{11} but not very efficiently with the LP_{12} and LP_{13}. Between these two extreme cases there is an intermediate region in which the fundamental mode is well guided but not the cladding modes. In this region the best mode overlap is produced between the fundamental mode LP_{01} and the first lobe of the higher order cladding modes LP_{13} and LP_{12}. This region is illustrated in Figure 5, which shows the radial dependent part of the field patterns $\gamma_{nk}(r,V)$ for a V-value of 2. As we will see, most of our AO experiments have been carried out in this intermediate region.

3. EXPERIMENTS

This section describes the experiments carried out to test the former theoretical predictions and also to demonstrate the potential of tapered fibres as complex profile AO filters.

3.1 EXPERIMENTAL SET-UP

The experiments described in this work typically consist of two stages: first, a controlled tapering of the fibre and, second, a test of its properties as AO filter. The fibre used in all the experiments was a standard telecommunication single-mode fibre, with a numerical aperture of 0.12, a core radius of 4 μm, and a cladding radius of 62.5 μm.

3.1.1 Tapering Stage

The fibres were tapered by means of the flame-brush technique [13,18-19], in which a point-like gas burner travels back and forth along a section of fibre that is symmetrically pulled from both ends. The shape of the taper is tailored by accurate control of the amplitude of the gas burner oscillations [19]. By gradually reducing the amplitude of these oscillations, monotonic nonuniform tapers with arbitrary shape can be fabricated.

The evolution of the tapered fibre during its fabrication can be rigorously described in terms of the spatial (η) and material (z) coordinates commonly used in fluid mechanics. The spatial coordinate $\eta(z,t)$ represents the position at time t of a transverse fibre slice that initially was situated at z. The partial differential equation satisfied by $\eta(z,t)$ can be shown to be (Appendix):

$$\frac{\partial^2 \eta}{\partial z\, \partial t} = \alpha \frac{\partial \eta}{\partial z} \delta(\eta - f(t)) \tag{16}$$

where α is the overall pulling speed of the fibre, δ is the Dirac delta, and f(t) is the instantaneous position of the point-like gas burner. The solution of (16) together with the law of mass conservation permits the calculation of the evolution of the fibre radius along the taper:

$$r(z) = r_o \left| \frac{\partial \eta}{\partial z} \right|^{-1/2} \tag{17}$$

where r_0 is the initial fibre radius. In the usual case in which the burner speed $|\dot{f}(t)|$ is much faster than the pulling speed α, equation (16) can be averaged in time to produce simple analytical solutions that predict the shape of tapers with great accuracy, as has already been described in the literature [19].

3.1.2 Acoustic wave excitation

The tapered fibre is then excited by an acoustic flexural wave generated by means of an electro-acoustic transducer. An electrical signal with frequency in the 1-1.5 MHz range is amplified and fed into a piezo-electric transducer (PZT) working in thickness mode. The PZT drives an acoustic horn of conic shape that concentrates the acoustic power into its apex, where the fibre is glued. The conic horn had a base with a radius of 6 mm and an axis of 4 mm. The electrical power consumption of the fabricated loss filters varies enormously with the taper radius and length of the devices. The typical consumption for fibres tapered in the 30-50 μm radius range is of the order of several hundred mW (1.3 W maximum), although this value could be drastically reduced in very thin tapers.

3.2 CHARACTERISATION OF AO RESONANCES IN UNIFORM TAPERS

The first experiments were intended to confirm the AO resonances theoretically predicted. A set of fibres was tapered to achieve uniform waists of radii varying from 30 to 50 μm and with a total length of 10 cm. The tapers were mounted under slight tension and the AO resonance wavelengths were monitored for each taper as a function of the acoustic frequency. The results for the $LP_{01} \leftrightarrow LP_{13}$, $LP_{01} \leftrightarrow LP_{12}$ and $LP_{01} \leftrightarrow LP_{11}$ interactions can be observed in Figures 6a, 6b and 6c respectively. The theoretical fits assume a fibre numerical aperture of 0.12, a cladding-core ratio of 62.5/4, and an applied tension of 0.9N.

The curves for the resonance wavelengths are in general double branched. Figure 7 shows the evolution of the coupling spectra for the 32.5μm radius taper as the acoustic frequency decreases from 1.31 to 1.24 MHz. The four resonances of Figure 7 correspond to the $LP_{01} \leftrightarrow LP_{11}$, $LP_{01} \leftrightarrow LP_{12}$ and the two branches of the $LP_{01} \leftrightarrow LP_{13}$ interaction respectively. It can be appreciated how the two resonance branches for the $LP_{01} \leftrightarrow LP_{13}$ interaction merge as the acoustic frequency decreases (Figure 6), disappearing finally for a low enough acoustic frequency. In these graphs, we can also compare the coupling efficiencies among the different interactions. The coupling between $LP_{01} \leftrightarrow LP_{13}$ is the one with highest efficiency in this range, while the $LP_{01} \leftrightarrow LP_{12}$ and $LP_{01} \leftrightarrow LP_{11}$ are much weaker. This behaviour can be explained with the help of Figure 4 and Equation (13). While the $LP_{01} \leftrightarrow LP_{13}$ interaction was operated near the V-value that gives maximum overlap for OI_3 ($V \approx 1.25$), the $LP_{01} \leftrightarrow LP_{12}$ and $LP_{01} \leftrightarrow LP_{11}$ were operated at V-values of about 1.5, resulting in a reduced mode overlap (Figure 4).

3.3 NONUNIFORM TAPERED FILTERS FOR GAIN FLATTENING APPLICATIONS

The variation of the fibre radius along a tapered structure gives rise to local AO resonances that translate into complex AO coupling spectra. The main application of these AO loss filters is the equalisation of the gain profile of optical fibre amplifiers. The great advantage of AO filters is that they permit dynamic compensation of gain saturation effects. In this section we will demonstrate a design consisting of two cascaded tapered AO filters that enables dynamic equalisation of fibre amplifiers.

Erbium doped fibre amplifiers (EDFA) exhibit a broadened gain spectrum due to Stark-splitting of the ground and metastable energy levels. The gain spectrum extends over more than 30nm and is composed of two main amplification peaks centred at around 1532 nm and 1550 nm respectively. In order to compensate the gain variations under saturation conditions it is convenient to control independently the attenuation in these two spectral regions.

Our equaliser design comprises two AO filters driven at the same acoustic frequency and spectrally shaped by their taper profile. The attenuation of each filter is controlled by the RF power of the driving signal. Each of the filters relies exclusively on the $LP_{01} \leftrightarrow LP_{13}$ AO interaction. Coherent noise that affects other schemes based on multi-frequency driven electro-acoustic transducers is negligible in this filter design.

The first AO filter is based on a nonuniform taper consisting of three uniform sections. Due to the fabrication procedure, the taper profile includes some transition regions between these uniform sections. The final fibre radius profile, shown in Figure8, can be theoretically predicted from reference [19] or alternatively, from Equations (16) and (17). The filter was designed by use of the model developed in Section 2.3 together with the experimental data obtained in Section 3.2. The first section had a length of 10mm and a radius of 40.2μm, the second was 20mm long and had a 38.4μm radius, and the last section was 60mm long and had a 37.2μm radius. The spectral response of the filter can be observed in Figure 9a. The coupling spectrum is asymmetric, with the long-wavelength side-lobe enhanced by the taper nonuniformity. This response can be explained as a result of interference among optical signals coupled at different sections of the taper. The second AO filter relies on a two stage taper, with a first section 12mm long and 42μm radius, and a second section 50mm long with a 41μm radius. Its spectral response is illustrated in Figure9b. The theoretical fit for both filters was calculated from Equation (12).

The two AO filters were slightly tuned by means of a small axial tension and then cascaded to combine their spectral responses and match the EDFA gain spectrum. The overall spectral response obtained when both filters were driven with electrical signals of 1.24 MHz and variable power levels is shown in Figure 9c. The overall filter exhibited low insertion losses, estimated to be less than 0.5 dB.

The potential of this AO filter as an equaliser was tested by flattening the amplified spontaneous spectrum (ASE) emitted by an EDFA with aluminium-germanosilica as host glass (Figure 10). The gain of the EDFA was saturated by an input signal from a DFB laser diode emitting at 1548 nm and set to several saturating power levels (-26dBm, -22 dBm, and -18.4dBm). As the saturating signal is increased, the spectral power density of the ASE decreased nonuniformly along the amplifier gain band. The overall decrease at 1550nm, 4 dB, was lower than that corresponding to 1532.5nm, 6.8dB. For each saturation level, the electrical power driving each of the two AO filters was optimised to give a maximally flat ASE spectrum. In all the cases, the fluctuations of the ASE spectrum were kept below 1dB for a wavelength range of 30nm (Figure 10).

The AO filter response time depends both on the dimensions of the device and the acoustic wave group-velocity, which can be calculated from Equation 4. The response time of a typical device is about 50 μs. The total RF power consumption of the filter was of the order of 1W. This value could be reduced by improving the electro-acoustic conversion efficiency, which was far from optimum in our case. One of the potential advantages of the use of AO filters based on tapered fibres is precisely the requirement of lower RF driving powers than for untapered devices [10]. Finally, it has to be stressed that both AO filters were driven with only one electrical frequency (1.24MHz), in contrast to other multi-frequency schemes [15-16]. This approach reduces slightly the filter flexibility but can result in a more compact and simple AO filter implementation.

4. CONCLUSIONS

In this paper we have demonstrated that the taper profile can be regarded as a new degree of freedom to tailor the spectral characteristics of AO filters. The influence of the taper radius in the performance of AO loss filters has been characterised both theoretically and experimentally. We have studied the evolution of the acousto-optic resonances as the fibres are progressively tapered, clarifying the nature of the interacting modes and the magnitude of the coupling efficiencies among them. We have also shown the applicability of this type of filters for dynamic gain control and equalisation of fibre amplifiers. An equaliser consisting of two cascaded AO filters was designed to flatten the ASE from an EDFA, achieving a fluctuation smaller than 1dB for an spectral gain band of 30nm and different saturation conditions. The novelty of the present design with respect to previous approaches is that it only relies on the taper profile to spectrally tailor the filter. As the use of several driving frequencies can provide added flexibility to the design of AO filters, future devices could combine both degrees of freedom to achieve optimum designs with a minimum number of driving frequencies.

ACKNOWLEDGEMENTS

The authors would like to thank S.G. Farwell, D.O. Culverhouse and T. Birks for previous background work in this area, and H.S. Kim for helpful discussions. Carlos Alegria acknowledges financial support from the Portuguese "Fundacão para a Ciência e Tecnologia". The ORC is an EPSRC Interdisciplinary Research Centre.

APPENDIX

In this appendix we will derive Equation (16). The spatial coordinate $\eta(z,t)$ represents the position at time t of a transverse fibre slice that initially was situated at z, α is the overall pulling speed of the fibre, and f(t) is the instantaneous position of the flame. The derivative $\frac{\partial \eta}{\partial z}$ has the meaning of local expansion of the fibre. Let us assume that a fibre slice of small length L is situated at position η and that the flame is sweeping across it at a time t. The increase of the expansion factor $\frac{\partial\eta}{\partial z}$ after the flame has swept the slice can be calculated as:

$$\delta\frac{\partial\eta}{\partial z}=\begin{cases}\alpha\dfrac{\partial\eta}{\partial z}\dfrac{1}{|\dot{f}(t)|}, & \text{if } |\eta-f(t)|<L/2\\ 0 \quad , & \text{if } |\eta-f(t)|>L/2\end{cases} \tag{A1}$$

where $\dot{f}(t)$ is the instantaneous sweeping speed. Dividing in (A1) by the sweeping time along the slice δt $(=L/|\dot{f}(t)|)$ we obtain:

$$\frac{\delta}{\delta t}\frac{\partial\eta}{\partial z}=\begin{cases}\alpha\dfrac{\partial\eta}{\partial z}\dfrac{1}{L}, & \text{if } |\eta-f(t)|<L/2\\ 0 \quad , & \text{if } |\eta-f(t)|>L/2\end{cases} \tag{A2}$$

which is equivalent to (16) in the limit $L\rightarrow 0$.

REFERENCES

[1] W.P. Risk, G.S. Kino, H.J. Shaw. "Fiber-optic frequency shifter using a surface acoustic wave incident at an oblique angle". Optics Letters, Vol. 11, No. 2, pp. 115-117. February 1986.

[2] B.Y. Kim, J.N. Blake, H.E. Engan, H.J. Shaw. "All-fiber acousto-optic frequency shifter". Optics Letters, Vol. 11, No. 6, pp. 389-391. June 1986.

[3] J.N. Blake, B.Y. Kim, H.E. Engan, H.J. Shaw. "Analysis of intermodal coupling in a two-mode fiber with periodic microbends". Optics Letters, Vol. 12, No. 4, pp. 281-283. April 1987.

[4] H.E. Engan, B.Y. Kim, J.N. Blake, H.J. Shaw. "Propagation and optical interaction of guided acoustic waves in two-mode optical fibers". Journal of Lightwave Technology, Vol. 6, No. 3, pp.428-436. March 1988.

[5] H. Sabert, L. Dong, P.St.J. Russell. Versatile acousto-optical flexural wave modulator, filter and frequency shifter in dual-core fiber". International Journal of Optoelectronics. Vol. 7, No. 2, pp. 189-194 (1992).

[6] M. Berwick, C.N. Pannell, P.St.J. Russell, D.A. Jackson. "Demonstration of birefringent optical fibre frequency shifter employing torsional acoustic waves". Electronics Letters, Vol. 27, No. 9, pp. 713-715. April 1991.

[7] H.E. Engan. "Analysis of polarization-mode coupling by acoustic torsional waves in optical fibres". Journal Optical Society America A, Vol. 13, No. 1, pp. 112-118. January 1996.

[8] S.H. Yun, I.K. Hwang, B.Y. Kim. "All-fiber tunable filter and laser based on two-mode fiber". Optics Letters, Vol. 21, No. 1, pp. 27-29. January 1996.

[9] T.A. Birks, P.St.J. Russell, D.O. Culverhouse. "The acousto-optic effect in single-mode fiber tapers and couplers". Journal of Lightwave Technology, Vol. 14, No. 11, pp. 2519-2529. November, 1996.

[10] T.A. Birks, P.St.J. Russell, C.N. Pannell. "Low power acousto-optic device based on a tapered single-mode fiber". IEEE Photonics Technology Letters, Vol. 6, No. 6, pp. 725-727. June 1994.

[11] T.A. Birks, S.G. Farwell, P.St.J. Russell, C.N. Pannell. "Four-port fiber frequency shifter with a null taper coupler". Optics Letters, Vol. 19, No. 23, pp. 1964-1966. December 1994.

[12] D.O. Culverhouse, S.G. Farwell, T.A. Birks, P.St.J. Russell. "Four port fused taper acousto-optic devices using standard singlemode telecommunications fibre". Electronics Letters, Vol. 31, No. 15, pp. 1279-1280. July 1995.

[13] S.G. Farwell, D.O. Culverhouse, T.A. Birks, P.St.J. Russell. "Low-loss all-fibre amplitude modulator at 1.55 μm". Electronics Letters, Vol. 32, No. 6, pp. 577-578. March 1996.

[14] T.A. Birks, D.O. Culverhouse, S.G. Farwell, P.St.J. Russell. "2X2 Single-mode fiber routing switch". Optics Letters, Vol. 21, No. 10, pp. 722-724. May 1996.

[15] H.S. Kim, S.H. Yun, I.K. Kwang, B.Y. Kim. "All-fiber acousto-optic tunable notch filter with electronically controllable spectral profile". Optics Letters, Vol. 22, No. 19, pp. 1476-1478. October 1997.

[16] H.S. Kim, S.H. Yun, H.K. Kim, N. Park, B.Y. Kim. "Actively gain-flattened erbium-doped fiber amplifier over 35 nm by using all-fiber acoustooptic tunable filters". IEEE Photonics Technology Letters, Vol. 10, No. 6, pp. 790-792. June 1998.

[17] A.M. Vengsarkar, J.R. Pedrazzani, J.B. Judkins, P.J. Lemaire, N.S. Bergano, C.R. Davidson. "Long-period fiber-grating-based gain equalisers". Optics Letters, Vol. 21, No. 5, pp. 336-338. March 1996.

[18] F. Bilodeau, K.O. Hill, S. Faucher, D.C. Johnson. "Low-loss highly overcoupled fused couplers: fabrication and sensitivity to external pressure". Journal of Lightwave Technology, Vol. 6, No. 10, pp. 1476-1482. October 1988.

[19] T.A. Birks, Y.W. Li. "The shape of fiber tapers". Journal of Lightwave Technology, Vol. 10, No. 4, pp. 432-438. April 1992.

FIGURE CAPTIONS

Figure 1. Schematic of the acousto-optic filter based on a tapered optical fibre.

Figure 2. Dispersion of the beatlength for the first three pair of modes as a function of the V number. The beatlength has been normalised against the fibre core radius a.

Figure 3. Resonance wavelengths for the three AO interactions as a function of the taper radius b with the acoustic frequency as parameter. The acoustic frequencies were 1.15MHz, 1.25 MHz and 1.35MHz, with the lowest frequency corresponding to the inner curve of each set.

Figure 4. Overlap integral OI_m for the three AO interactions under study as a function of the V number.

Figure 5. Radial part of the normalised LP_{01}, LP_{11}, LP_{12} and LP_{13} fields for V=2.

Figure 6. Experimental and theoretical resonance wavelengths as a function of the acoustic frequency for several taper radius. 5a corresponds to the interaction $LP_{01}\leftrightarrow LP_{13}$, 5b to $LP_{01}\leftrightarrow LP_{12}$, and 5c to $LP_{01}\leftrightarrow LP_{11}$.

Figure 7. Evolution of the coupling spectrum corresponding to the 32.5μm radius taper as the acoustic frequency decreases: (a) 1.31 MHz, (b) 1.30 MHz, (c) 1.28 MHz, (d) 1.24 MHz.

Figure 8. Radius profile for the first tapered AO filter.

Figure 9. Spectral response for the first (8a) and second (8b) AO filters, and combined response when both filters are cascaded (8c). The broken lines (--) represent theoretical fits.

Figure 10. Flattened ASE spectrum for several levels of an input saturating signal (9a: No saturating signal, 9b: -26 dBm, 9c: -22 dBm, and 9d: -18.4dBm).

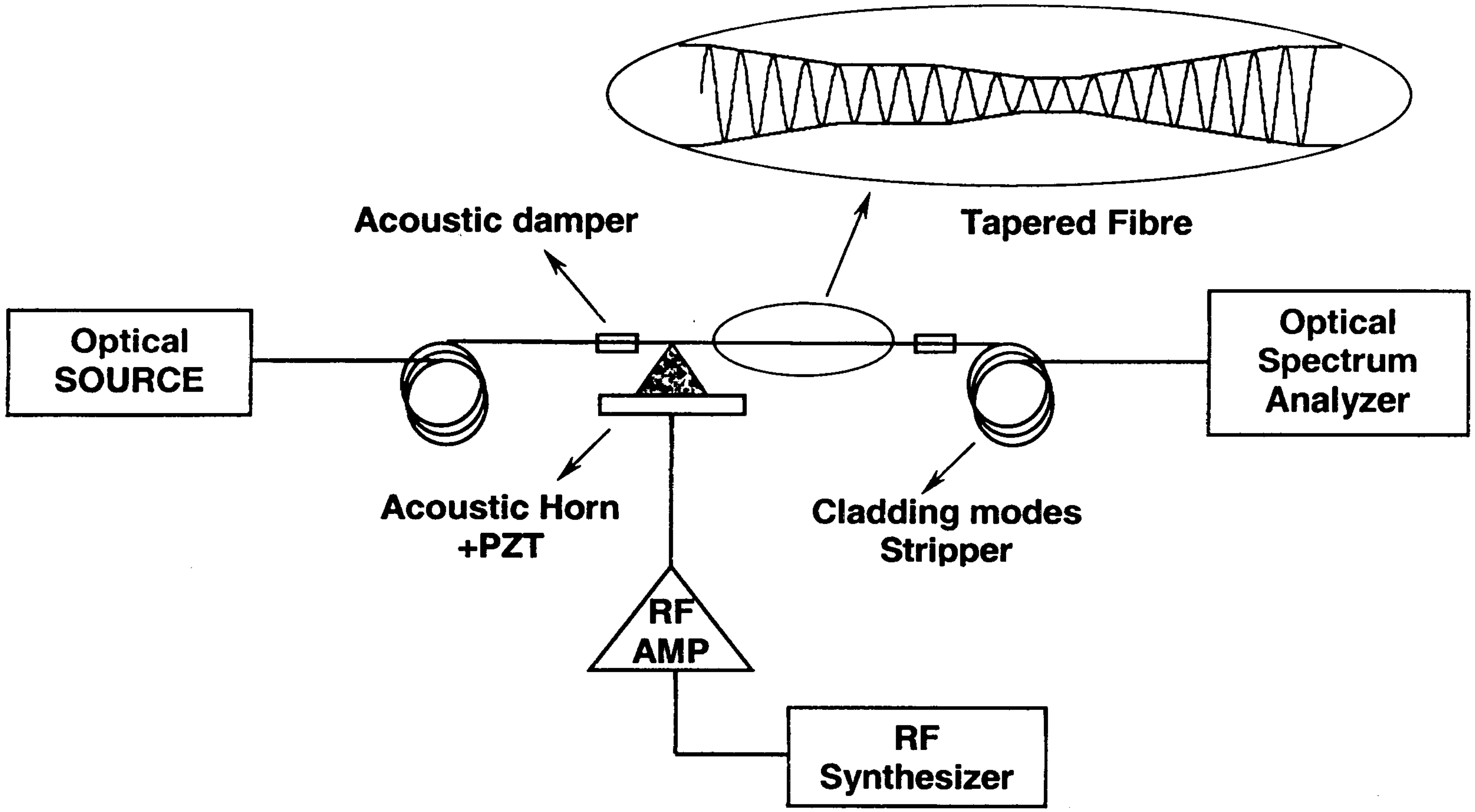
Acoustic damper
Tapered Fibre
Optical
SOURCE
Optical
Spectrum
Analyzer
Acoustic Horn
+PZT
Cladding modes
Stripper
RF
AMP
RF
Synthesizer

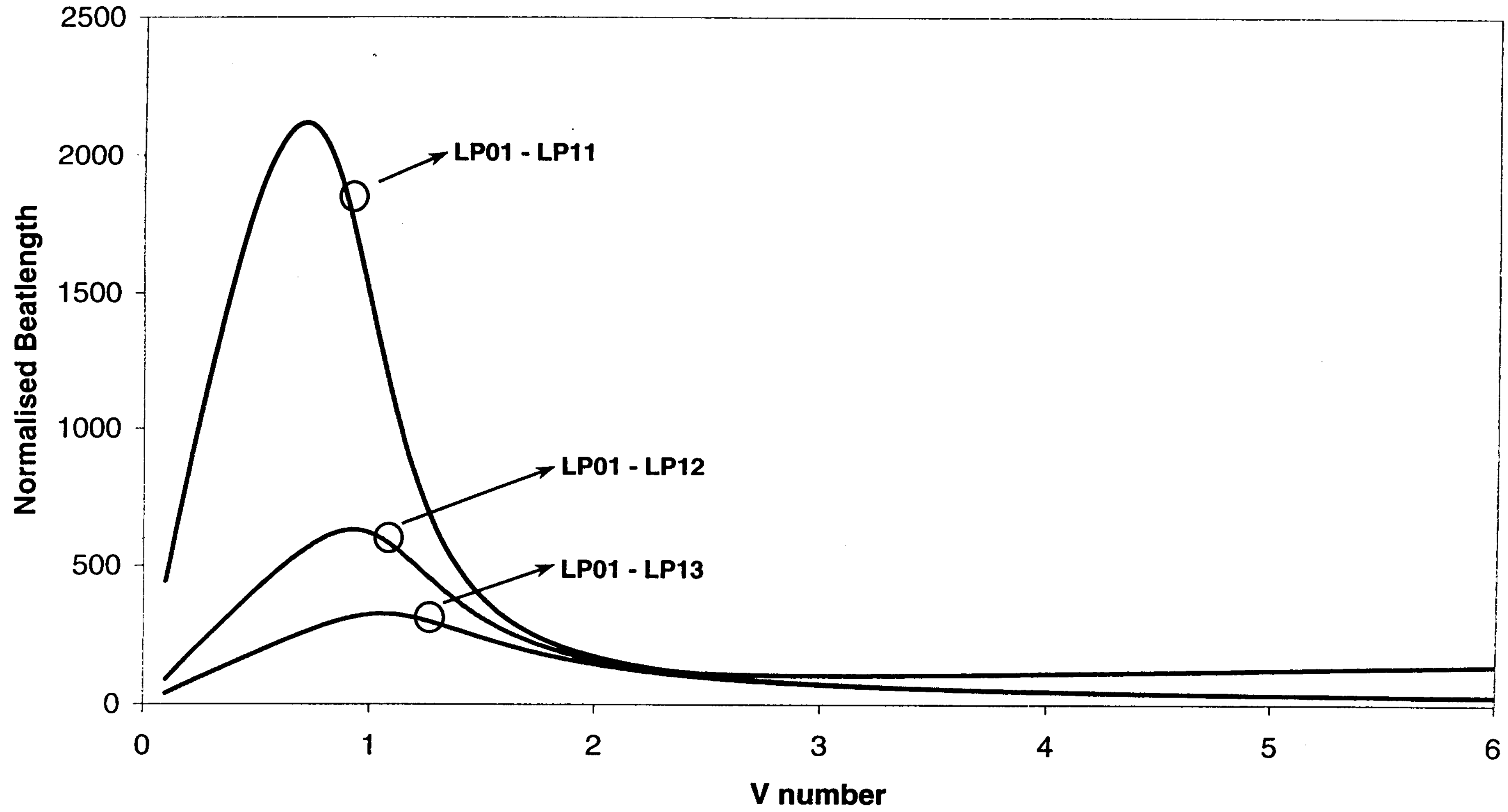

2500
2000
1500
1000
500
0
Normalised Beatlength
LP01 - LP11
LP01 - LP12
LP01 - LP13
0
1
2
3
4
5
6
V number

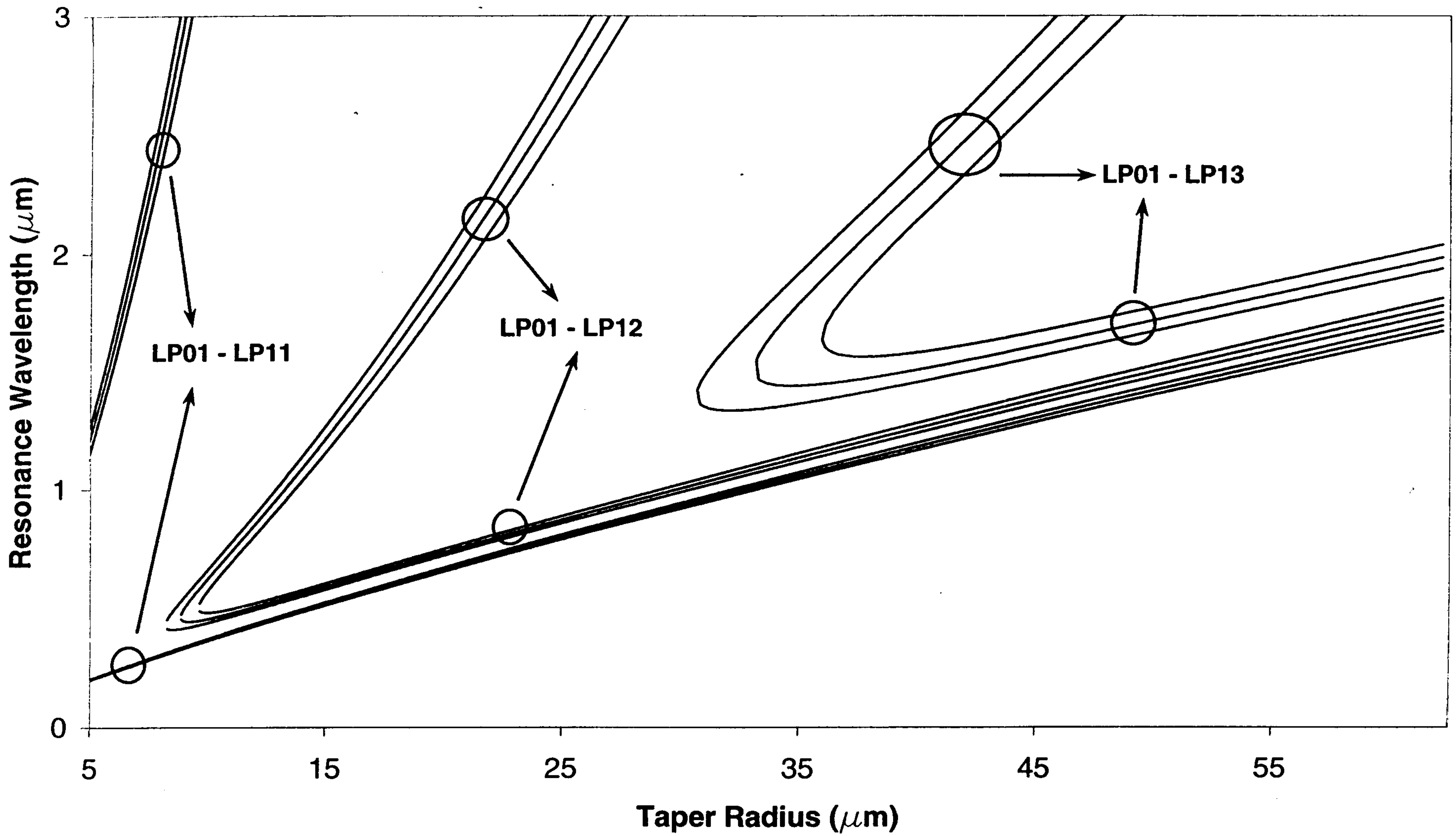
LP01 - LP11
LP01 - LP12
LP01 - LP13
Resonance Wavelength (μm)
Taper Radius (μm)
0
1
2
3
5
15
25
35
45
55

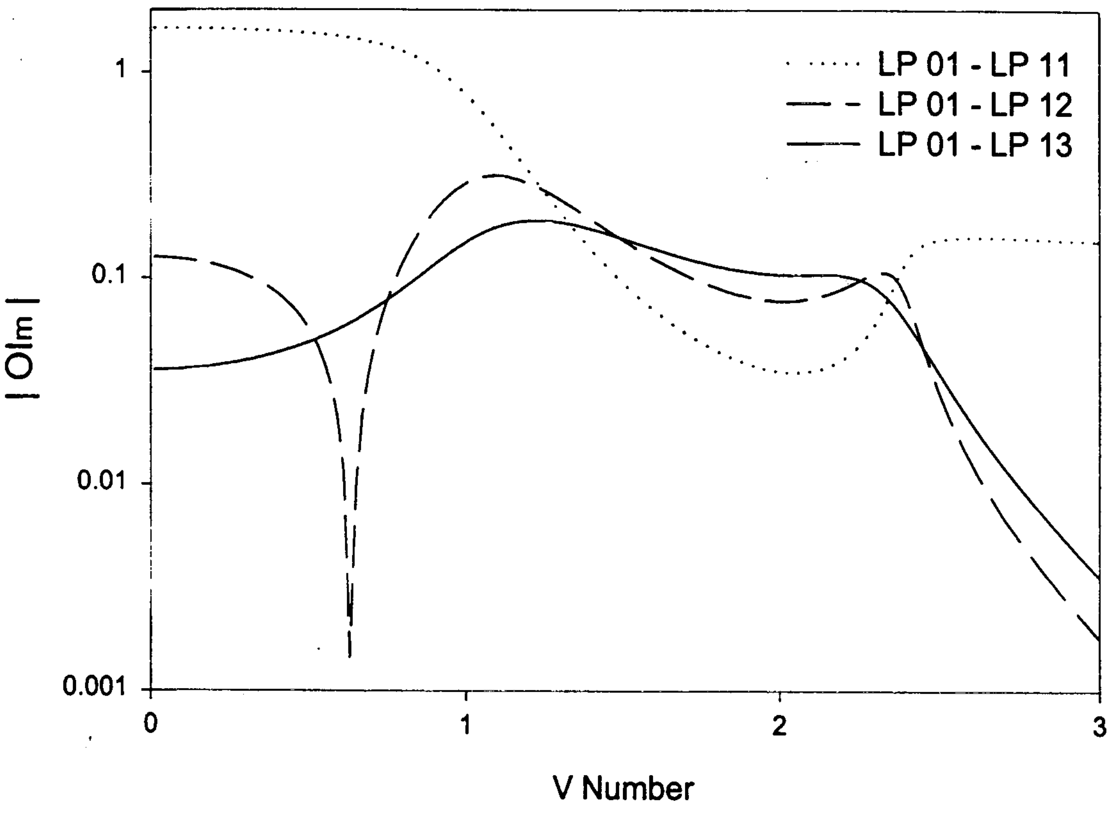
LP 01 - LP 11
LP 01 - LP 12
LP 01 - LP 13
1
0.1
0.01
0.001
| Olm |
0
1
2
3
V Number

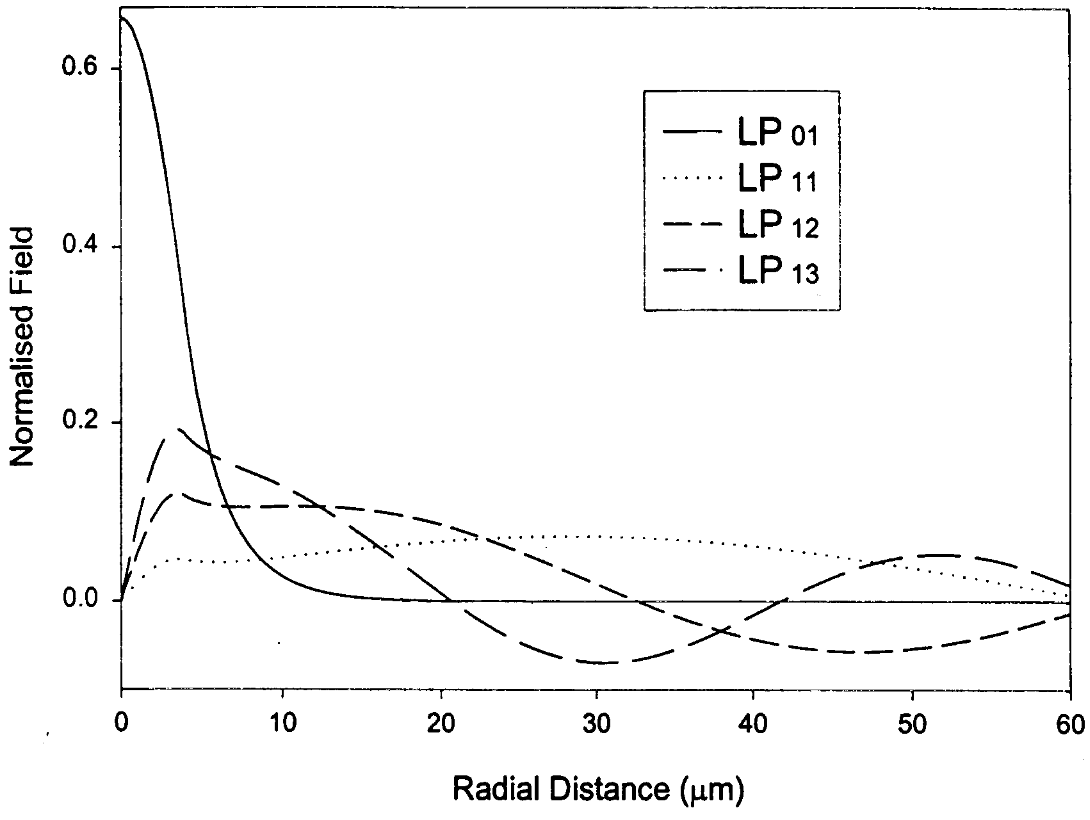

0.6
0.4
0.2
0.0
Normalised Field
LP 01
LP 11
LP 12
LP 13
0
10
20
30
40
50
60
Radial Distance (μm)

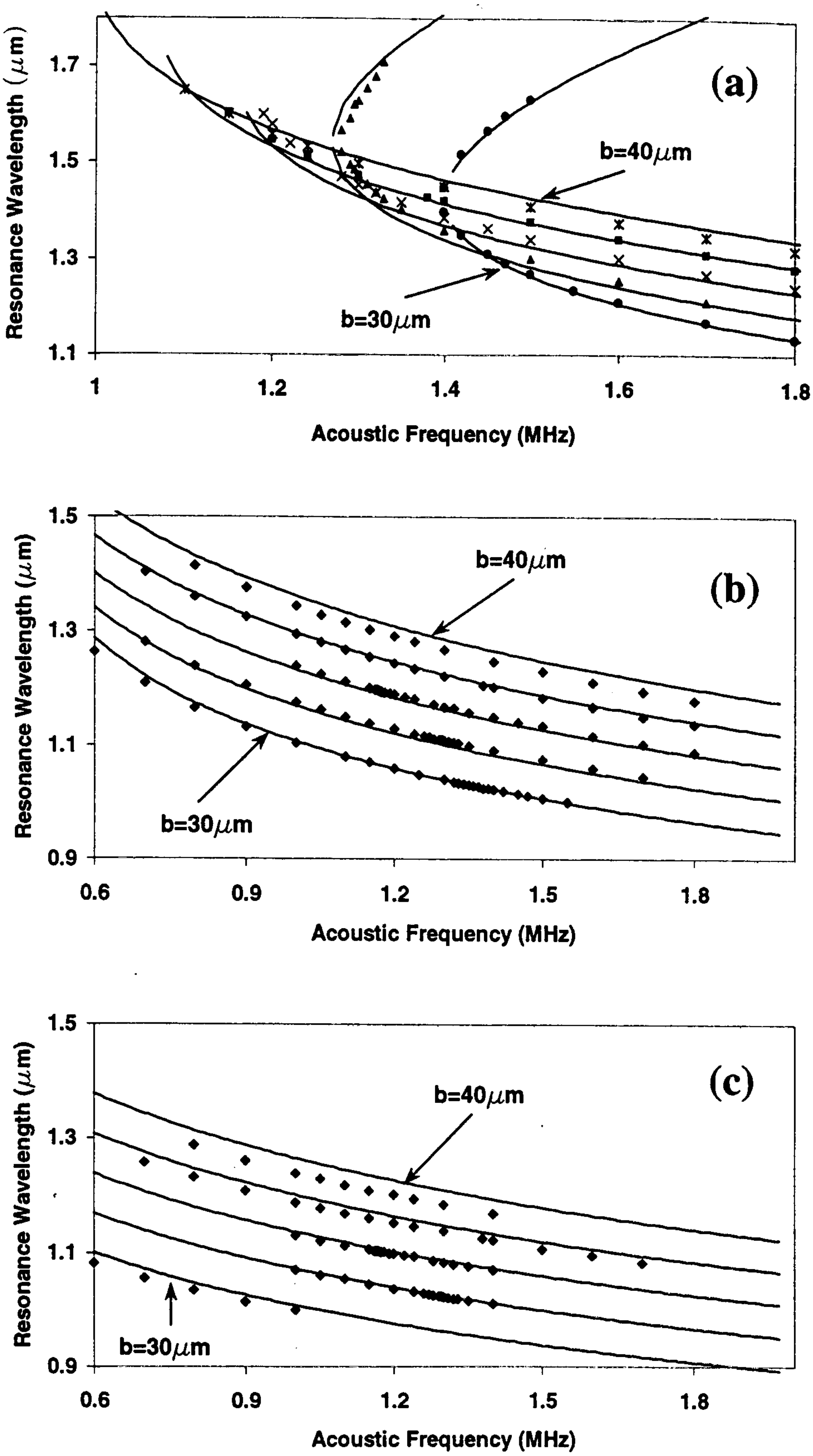

(a)
Resonance Wavelength (μm)
1.7
1.5
1.3
1.1
b=40μm
b=30μm
1
1.2
1.4
1.6
1.8
Acoustic Frequency (MHz)
(b)
Resonance Wavelength (μm)
1.5
1.3
1.1
0.9
b=40μm
b=30μm
0.6
0.9
1.2
1.5
1.8
Acoustic Frequency (MHz)
(c)
Resonance Wavelength (μm)
1.5
1.3
1.1
0.9
b=40μm
b=30μm
0.6
0.9
1.2
1.5
1.8
Acoustic Frequency (MHz)

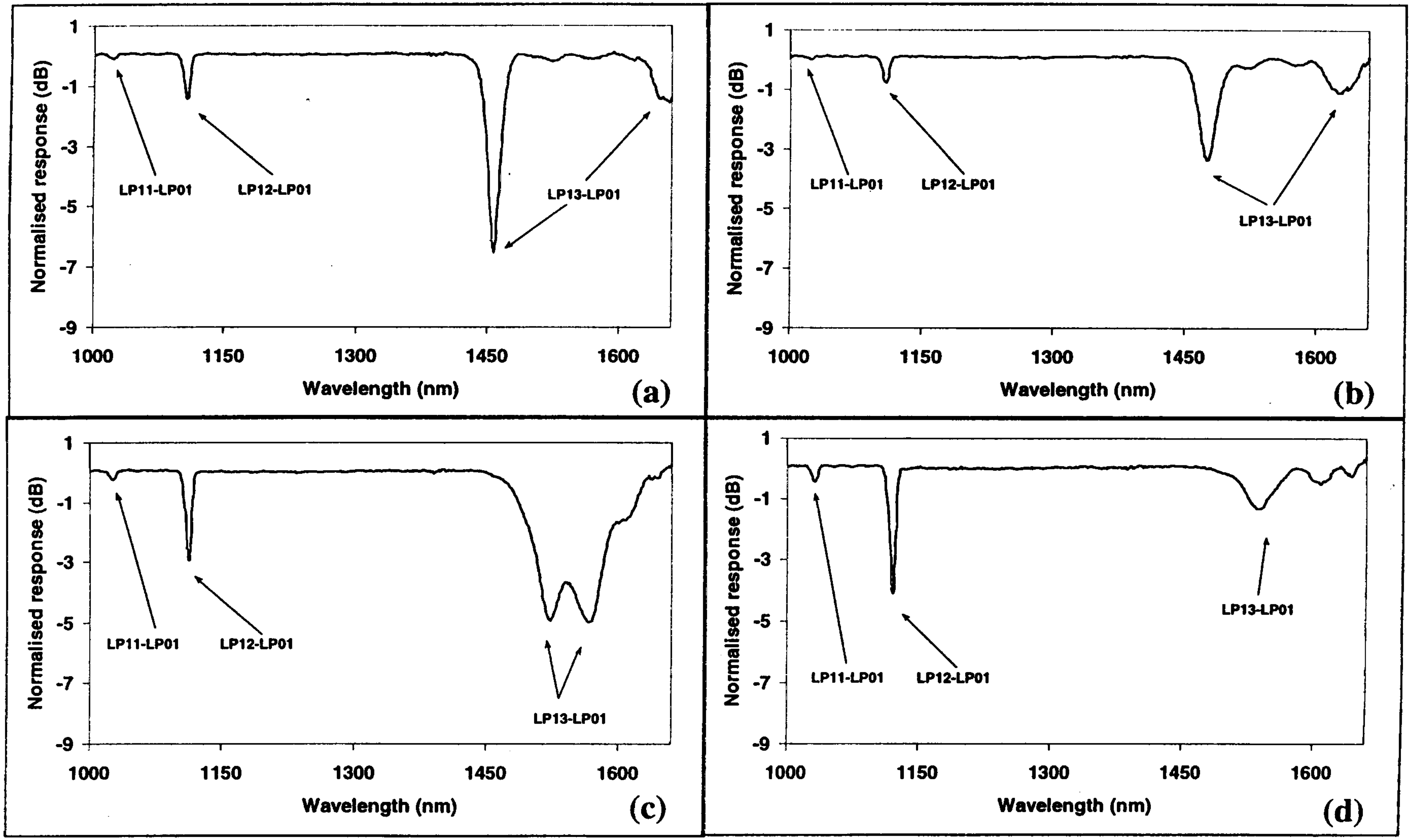
Normalised response (dB)
1
-1
-3
-5
-7
-9
1000
1150
1300
1450
1600
Wavelength (nm)
LP11-LP01
LP12-LP01
LP13-LP01
(a)
(b)
(c)
(d)

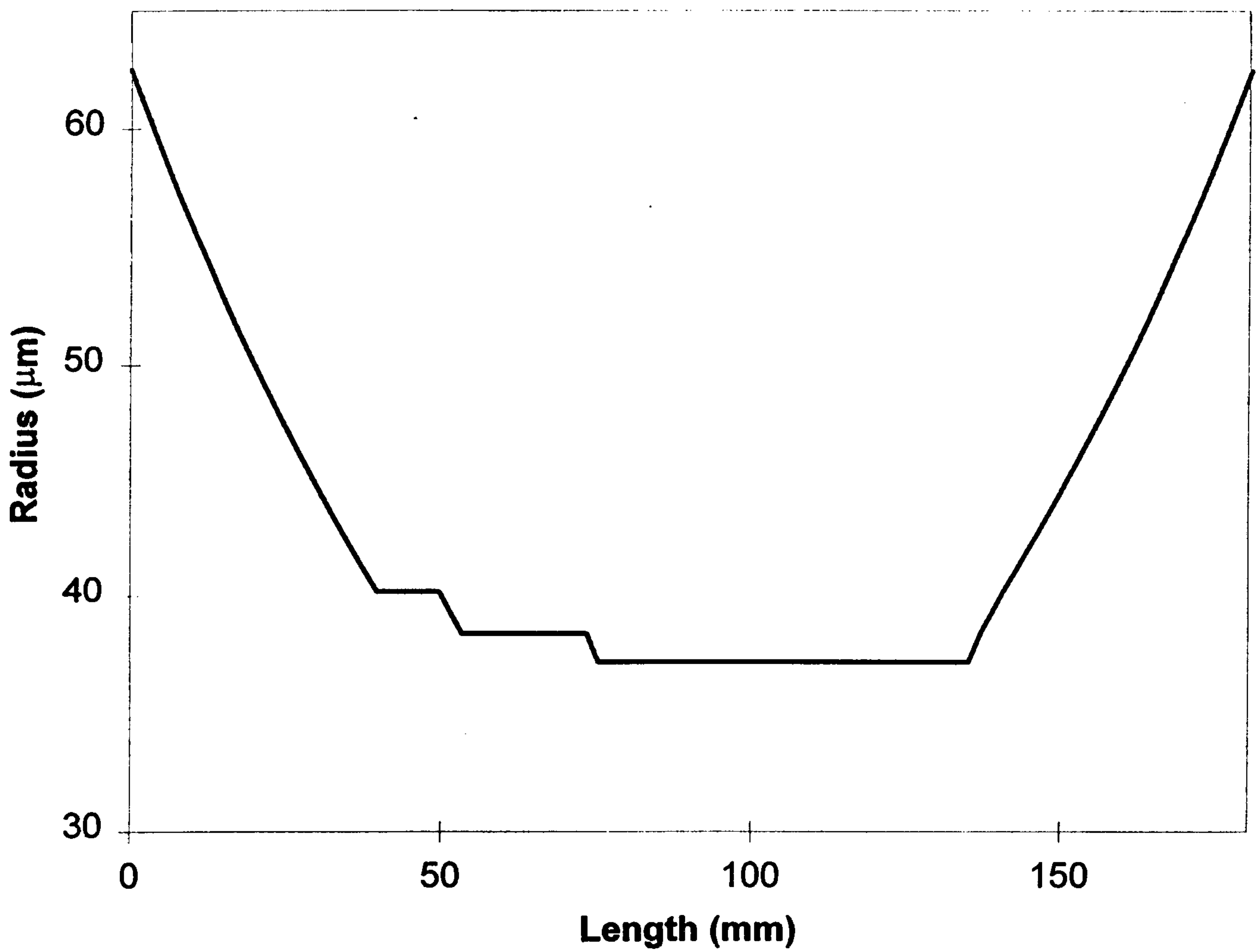
60
50
40
30
Radius (μm)
0
50
100
150
Length (mm)

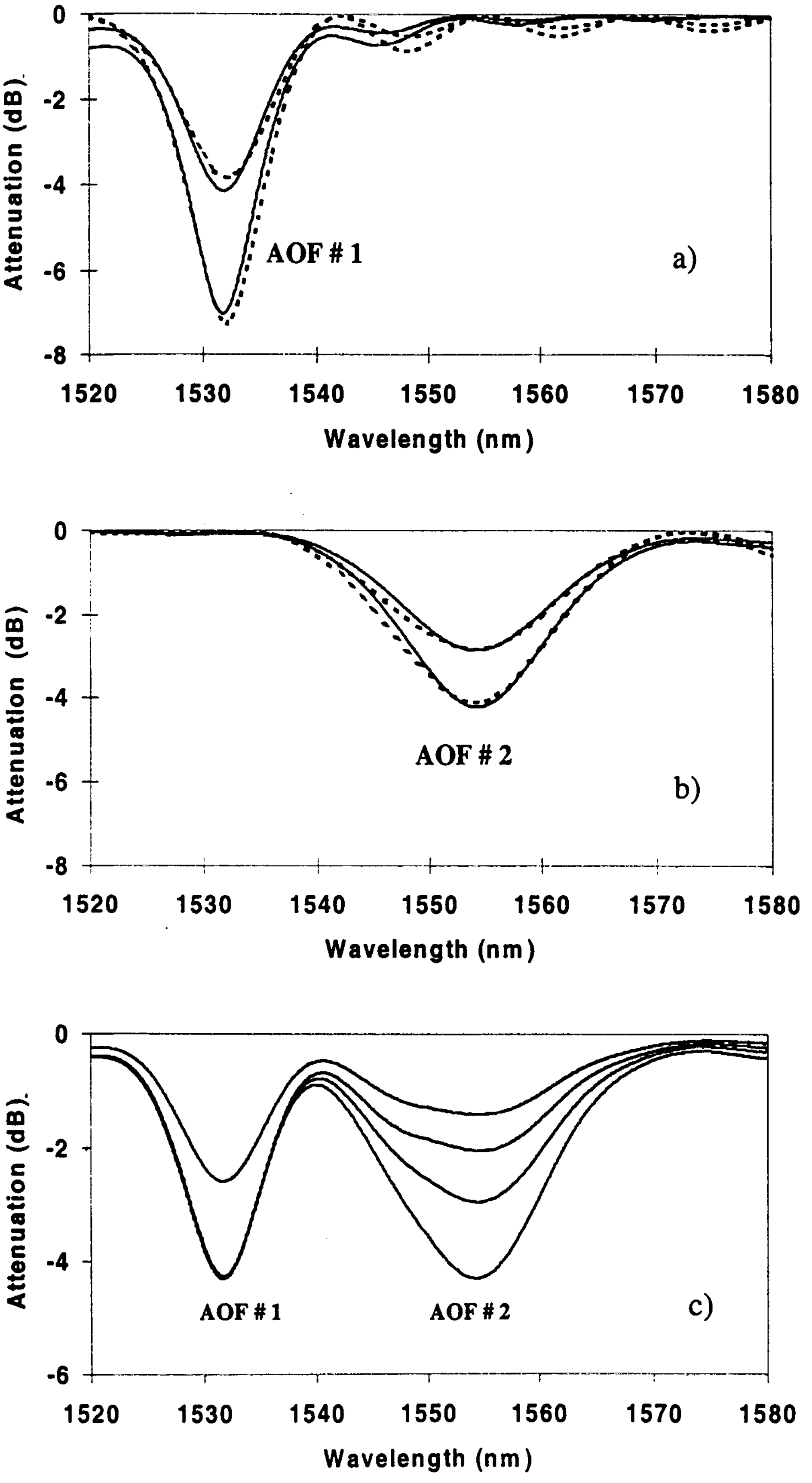
0
-2
-4
-6
-8
Attenuation (dB)
AOF # 1
a)
1520
1530
1540
1550
1560
1570
1580
Wavelength (nm)
0
-2
-4
-6
-8
Attenuation (dB)
AOF # 2
b)
1520
1530
1540
1550
1560
1570
1580
Wavelength (nm)
0
-2
-4
-6
Attenuation (dB)
AOF # 1
AOF # 2
c)
1520
1530
1540
1550
1560
1570
1580
Wavelength (nm)

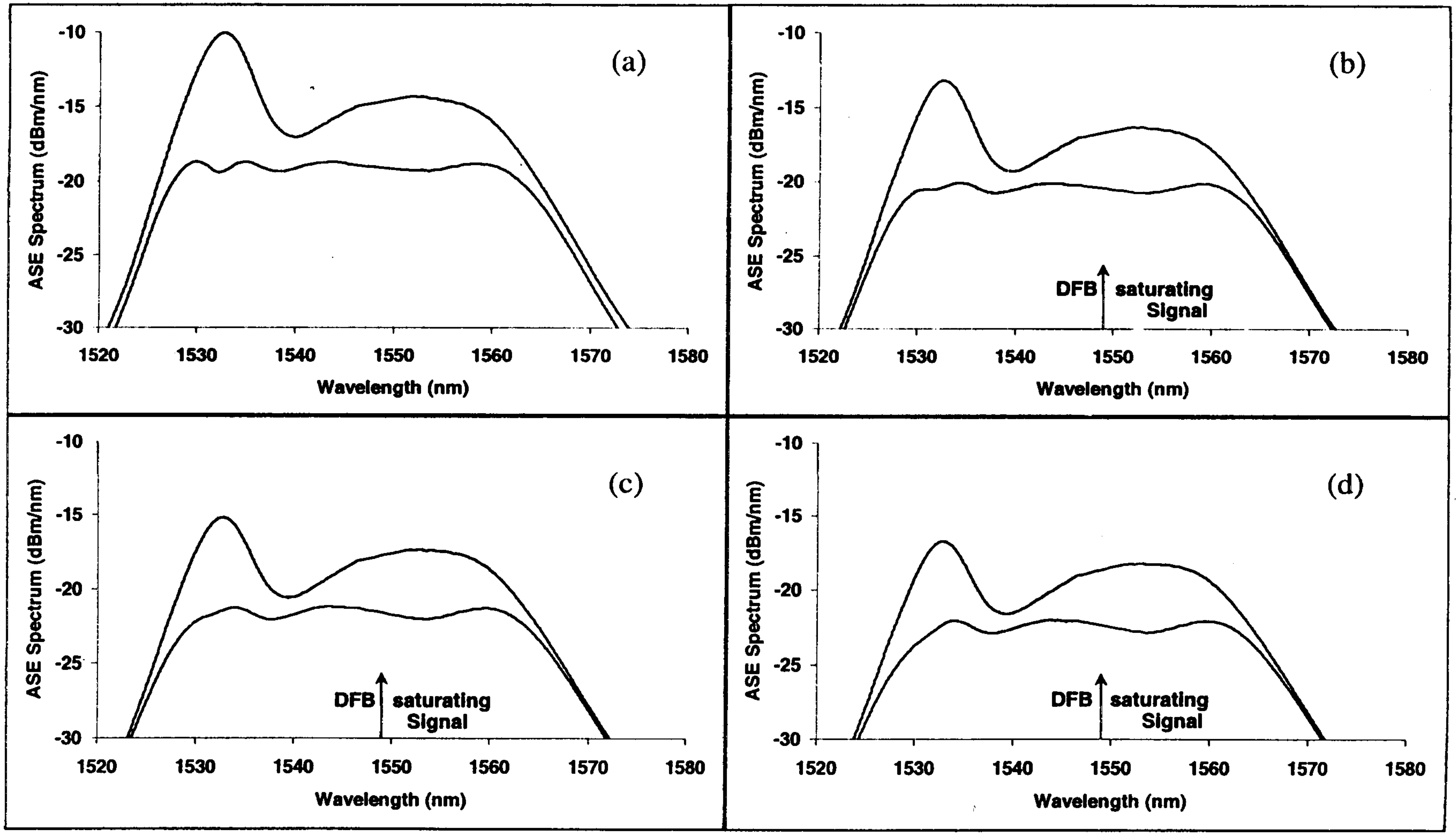
(a)
(b)
(c)
(d)
ASE Spectrum (dBm/nm)
-10
-15
-20
-25
-30
1520
1530
1540
1550
1560
1570
1580
Wavelength (nm)
DFB
saturating
Signal